Improving Cubic EOSs Near the Critical Point by a Phase-Space Cell Approximation

Francesco Fornasiero, Leo Lue, and Alberto Bertucco
Istituto Impianti Chimici, Università di Padova, Via Marzolo 9, I-35131 Padova, Italy

Cubic equations of state (EOSs) are widely used to model the thermodynamic properties of pure fluids and mixtures. However, because they fail to account for the long-range fluctuations existing in a fluid near the critical point, they do not accurately predict the fluid properties in the critical region. Recently, an approximate renormalization group method was developed that can account for these fluctuations. A similar method is applied to provide corrections to a generalized cubic EOS for pure fluids, which is able to represent all classic cubic EOSs. The proposed approach requires two additional parameters: $\bar{c}_{RG}$ and Δ. The value of $\bar{c}_{RG}$ is correlated to experimental critical compressibility data, while Δ is set equal to 1. The method is applied to predict the saturated liquid density of fluids of different polarity, and the corrections to the original EOS are found to significantly improve the predictions of this property both far from and close to the critical point. Finally, a correlation is presented for the direct evaluation of the parameter $\bar{c}_{RG}$ from the value of the critical compressibility factor.

Introduction

Cubic equations of state (EOSs) are widely used in process design and simulation to calculate thermodynamic properties of pure fluids and mixtures because they are simple, accurate, and flexible at the same time. These equations are able to describe quantitatively both equilibrium and volumetric properties of fluids away from the critical point; however, they give a poor description near the critical point (Goldenfeld, 1996). This failure is inherent to the model, since cubic EOSs exhibit mean field critical behavior and fail to take into account long wavelength density fluctuations, which are very important near the critical point.

In engineering applications, it is desirable to have an accurate EOS for representing the behavior of pure fluids and mixtures both close to and far from the critical point. One method for obtaining such an EOS is to "splice" together the known behavior of fluids asympotically close to the critical point with an equation of state (as a cubic EOS) that works well far away from the critical region. A model using this approach is typically referred to as a crossover EOS. This model has been applied recently to pure fluids as well as to binary mixtures (Kiselev, 1998a; Kiselev and Friend, 1998; Anisimov et al., 1998a,b).

An alternate approach is that proposed by Wilson (1971a,b), who introduced the phase-space cell approximation for the qualitative analysis of the behavior of systems near the critical point; this procedure leads to an EOS with nonclassic exponents, close to those observed experimentally. White and coworkers (Salvino and White, 1992; White and Zhang, 1993, 1995, 1997) have extended the range of applicability of Wilson's method to regions of the phase diagram beyond the asymptotic critical regime. The resulting theory is accurate and computationally efficient in a broad region around the critical point. Recently, Lue and Prausnitz (1998a,b) extended this approach to a larger region around the critical point.

The purpose of this work is to improve the volumetric behavior of cubic EOSs for pure fluids in the vicinity of the critical point. In order to incorporate effects of fluctuations, we applied the White's approximate renormalization group (RG) method to a generalized cubic EOS that can represent all classic cubic EOSs.

The proposed RG method requires two additional parameters, $\bar{c}_{RG}$ and Δ; the parameter Δ is set equal to 1, while the parameter $\bar{c}_{RG}$ is chosen to reproduce the experimental criti-

Correspondence concerning this article should be addressed to L. Lue at his present address: Physical and Chemical Properties Division, 838.08, National Institute of Standards and Technology, 325 Broadway, Boulder, CO 80303.

cal compressibility. In this way, it is possible to minimize the errors of saturated liquid density calculations. The results obtained are very satisfactory for all compounds considered, which span from low polar to high polar ones. In addition, since the correction is made on the specific Helmholtz energy, the calculation of all other thermodynamic properties is expected to be improved as well.

This article is organized as follows. After briefly reviewing the generalized cubic EOS, from which the van der Waals (vdW), Redlich–Kwong–Soave (RKS) and Peng–Robinson (PR) EOSs can be derived, we point out the limits of such models to reproduce volumetric properties of pure fluids near the critical point. Then we review the basic equations of the RG method, and discuss the details of their implementation. Further, we describe the procedure for evaluating parameters of the generalized EOS in the framework of the RG method. Finally, the effectiveness of the proposed approach is discussed and tested against experimental data of saturated liquid densities of pure fluids. A correlation is presented for the direct evaluation of the parameter $\bar{c}_{RG}$ from the value of the critical compressibility factor.

Generalized Cubic EOS

Theory

As outlined by Soave et al. (1999), the generalized cubic EOS has an algebraic form similar to the RKS EOS:

$$P = \frac{RT}{(v+c)-b} - \frac{a(T)}{(v+c)(v+c+d)} \qquad \text{with} \quad a(T) = a_c\alpha(T), \quad (1)$$

where v, P, T are molar volume, pressure, and temperature, respectively; R is the universal gas constant; a and b are the attractive and repulsive parameters; a_c is the value of a at the critical point; and $\alpha(T)$ is a function of temperature used to exactly reproduce vapor pressure data (Soave, 1986). Note that Eq. 1 takes into account the volume shift according to Peneloux et al. (1982) through parameter c, which does not affect vapor pressure calculations, and that different values of d correspond to different forms of the EOS (i.e., different cubic EOSs). The parameters a_c, b, c, and d can be expressed for each compound as functions of the critical temperature and pressure T_c and P_c:

$$a_c = \Omega_a\frac{R^2T_c^2}{P_c}; \qquad b = \Omega_b\frac{RT_c}{P_c}$$

$$c = \Omega_c\frac{RT_c}{P_c}; \qquad d = \Omega_d\frac{RT_c}{P_c}, \quad (2)$$

where Ω_a, Ω_b, and Ω_d are constants for a given EOS, and Ω_c is independent of temperature and pressure but is a function of the fluid identity. Once the cubic EOS is selected by setting a value of Ω_d, the values of Ω_a, Ω_b, and Ω_c can be calculated by imposing the zero-slope tangency condition at $T = T_c$, $P = P_c$, and (for Ω_c only) one reference value of the liquid density. In this way, for example, it is possible to obtain the classic vdW, RKS, and PR EOS by using the values reported in Table 1.

Evaluation of parameters

It is convenient to write Eq. 1 in a dimensionless form:

$$(Z+C)^3 - (Z+C)^2\left(\frac{1}{B}+1-\frac{D}{B}\right)B + (Z+C)\left[\frac{A}{B}-\frac{D}{B}(1+B)\right]B - \frac{A}{B}B^2 = 0, \quad (3)$$

where A, B, C, and D are defined by

$$A = \frac{a_c\alpha(T_r)P}{R^2T^2} = \alpha(T_r)\Omega_a\frac{P_r}{T_r^2}$$

$$B = \frac{bP}{RT} = \Omega_b\frac{P_r}{T_r}$$

$$C = \frac{cP}{RT} = \Omega_c\frac{P_r}{T_r}$$

$$D = \frac{dP}{RT} = \Omega_d\frac{P_r}{T_r}. \quad (4)$$

In Eqs. 4, P_r, T_r are the reduced pressure and temperature. Note that

$$\frac{A}{B} = \frac{\Omega_a}{\Omega_b}\left(\frac{\alpha(T_r)}{T_r}\right) \quad (5)$$

is pressure independent and

$$\frac{D}{B} = \frac{\Omega_d}{\Omega_b} \quad (6)$$

is constant at fixed Ω_d. In dimensionless variables, the fugacity coefficient is expressed by

$$\ln\varphi = Z - 1 - \ln(Z+C-B) + \frac{A}{D}\ln\left(\frac{Z+C}{Z+C+D}\right). \quad (7)$$

Table 1. Values of Parameters of the Generalized Cubic EOS to Obtain the Classic Cubic Equations of State

	b	d	c	Ω_a	Ω_b	Ω_d
Van der Waals	b_{vdW}	0	c_{vdW}	0.42188	0.125	0
Redlich–Kwong–Soave	b_{RKS}	b_{RKS}	c_{RKS}	0.42748	0.08664	0.08664
Peng–Robinson	$(2-\sqrt{2})b_{\text{PR}}$	$2\sqrt{2}\,b_{\text{PR}}$	$c_{\text{PR}} - (\sqrt{2}-1)b_{\text{PR}}$	0.45724	0.07780	0.22003

The value of α for a given $T < T_c$ is determined to exactly reproduce vapor pressure data: this is achieved by simultaneously solving Eq. 3 for both the liquid and vapor phases, in addition to the isofugacity condition:

$$\ln \varphi^V = \ln \varphi^L. \tag{8}$$

The parameter c (or Ω_c) is calculated by solving Eq. 1 with respect to c on the basis of one experimental liquid density datum at known P, T conditions. We have used either the value at $P = 1$ atm and $T = 293$ K, or the saturated density value at the lowest temperature of validity of the vapor pressure equation (if it was higher than 293 K), or the one at the boiling temperature at $P = 1$ bar (if the boiling temperature was lower than 293 K). The parameter c could be obtained also from the critical compressibility factor, Z_c.

Limit of cubic equation of state

In Figure 1 the percent error in the calculation of the saturated liquid density of propylene is shown for the RKS EOS at different values of the parameter c. At best, the accuracy of the prediction is acceptable only up to $T_r = 0.75$, and the error increases sharply in the vicinity of the critical point. This is a general, yet unacceptable, behavior of all cubic EOS: the error usually becomes as high as 25–30% for nonpolar compounds, and it goes up also to 50% for polar ones when approaching the critical point.

Renormalization Group Correction

To our purpose, it is useful to rewrite the generalized cubic EOS in terms of different dimensionless variables:

$$\bar{P} = \frac{\bar{T}\bar{\rho}}{1+(\bar{c}-1)\bar{\rho}} - \frac{\bar{\rho}^2}{(1+\bar{c}\bar{\rho})\left[1+(\bar{c}+\bar{d})\bar{\rho}\right]}, \tag{9}$$

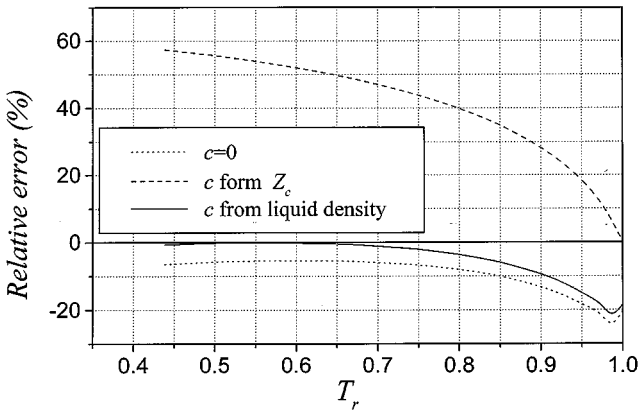

Figure 1. Percent error in the calculation of saturated liquid density of propylene for RKS EOS for different *c* parameter values.

(i) $c = 0$ (dotted line); (ii) c calculated fitting Z_c (dashed line); (iii) c calculated fitting experimental liquid density at $P = 1$ atm and $T = 225.4$ K (solid line).

where ρ is the molar density ($\rho = 1/v$) and the dimensionless variables are defined by

$$\bar{\rho} = b\rho; \qquad \bar{T} = \frac{bRT}{a(T)}; \qquad \bar{P} = \frac{b^2 P}{a(T)}$$

$$\bar{f} = \frac{b^2}{a(T)} f; \qquad \bar{c} = \frac{c}{b}; \qquad \bar{d} = \frac{d}{b}. \tag{10}$$

To include the contribution of long-wavelength fluctuations, we refer to the Helmholtz energy. In fact, according to the global RG method proposed by White and Zhang (1993, 1995), the specific Helmholtz energy (or Helmholtz energy density) f of a fluid is obtained by correcting the value of f as calculated by the mean-field approach.

In the present work we use the generalized cubic EOS summarized in the previous section and dimensionless variables defined by Eq. 10; therefore, the mean-field values of the chemical potential and of the specific Helmholtz energy, which will be indicated by $\bar{\mu}_{\text{cubic}}$ and $\bar{f}_{\text{cubic}}$, respectively, can be expressed by (see Appendix A for details):

$$\bar{\mu}_{\text{cubic}} = \bar{\mu}^0 - \bar{T}\ln\left[1+(\bar{c}-1)\bar{\rho}\right] + \frac{1}{d}\ln\left[\frac{1+\bar{c}\bar{\rho}}{1+(\bar{c}+\bar{d})\bar{\rho}}\right]$$

$$-\frac{\bar{\rho}}{(1+\bar{c}\bar{\rho})\left[1+(\bar{c}+\bar{d})\bar{\rho}\right]} + \bar{T}\ln\bar{T}\bar{\rho} - \frac{(\bar{c}-1)\bar{\rho}\bar{T}}{1+(\bar{c}-1)\bar{\rho}} \tag{11}$$

$$\bar{f}_{\text{cubic}} = \bar{\rho}\left\{\bar{\mu}^0 - \bar{T}\ln\left[1+(\bar{c}-1)\bar{\rho}\right] + \frac{1}{\bar{d}}\ln\left[\frac{1+\bar{c}\bar{\rho}}{1+(\bar{c}+\bar{d})\bar{\rho}}\right] + \bar{T}\left[\ln\left(\bar{T}\bar{\rho}\right)-1\right]\right\}. \tag{12}$$

Note that the dimensionless form of the EOS is convenient because, in this way, the two parameters a and b do not appear in the calculation procedure.

At a given temperature, the RG correction to the specific Helmholtz energy is evaluated for each value of density between ρ and $\rho_{\max}$, where $\bar{\rho}_{\max} = 1/(1-\bar{c})$ is the maximum permissible value of the dimensionless fluid density according to Eq. 12; 400 equally spaced points are considered, and a cubic spline function is used to get a continuous isotherm.

For each density value, the method has to be applied in an iterative manner, where each successive iteration includes the effects of density fluctuations of longer and longer wavelengths. The algorithm used in this work, derived from that by Salvino and White (1992), can be summarized as follows:

$$\begin{cases} \bar{f}_n = \bar{f}_{n-1} + \delta\bar{f}_n \\ \delta\bar{f}_n = -K_n \ln\left(\dfrac{Q_{n,s}}{Q_{n,l}}\right) \end{cases} \qquad 0 \le \bar{\rho} < \bar{\rho}_{\max}, \tag{13}$$

where

$$\begin{cases} K_n = \dfrac{\bar{T}}{2^{3n}\bar{c}_{RG}} \\ Q_{n,i} = \displaystyle\int_0^{\min[\bar{\rho},\,\bar{\rho}_{\max}-\bar{\rho}]} \exp\left\{-\frac{G_{n,i}}{K_n}\right\} dx & i = s, l \\ G_{n,i} = \dfrac{1}{2}\left[\tilde{f}_{n,i}(\bar{\rho}+x) + \tilde{f}_{n,i}(\bar{\rho}-x)\right] - \tilde{f}_{n,i}(\bar{\rho}) & i = s, l \end{cases} \tag{14}$$

$$\begin{cases} \tilde{f}_{n,l} = \bar{f}_{n-1} - \bar{f}_{0,a} \\ \tilde{f}_{n,s} = \bar{f}_{n-1} - (2^{-2n}\Delta)\,\bar{f}_{0,a} \\ \bar{f}_0 = \bar{f}_{\text{cubic}} \\ \bar{f}_{0,a} = -\bar{\rho}^2. \end{cases} \tag{15}$$

Note that in Eqs. 13–15, s and l refer to the preceding and subsequent step within each iteration, and that $\bar{c}_{RG}$ and Δ are two additional parameters of the equation of state. Note also that the original algorithm of Salvino and White (1992) has been modified in two ways:

1. The correction to the free energy density is calculated in the whole density range $[0, \rho_{\max}]$, which was not the case in the original procedure; thus, the upper integration limit in Eq. 14 has been changed according to: $\rho \rightarrow \min[\rho, \rho_{\max} - \rho]$;

2. The starting point of calculation, $\bar{f}_0$, is the value given by the cubic EOS, from which the original long-wavelength contributions to the attractive term have been subtracted: this term is roughly expressed by $-\bar{\rho}^2$, in analogy with what is currently done for other EOSs (Salvino and White, 1992; White and Zhang, 1993; Lue and Prausnitz, 1998a,b).

By applying the previous relations, successive approximations of the free energy density ($\bar{f}_n$) to its true value ($\bar{f}_\infty$) are obtained, each containing the contribution of density fluctuations of larger and larger wavelengths. In all cases considered, we have seen that for $n > 5$, the value of $\bar{f}_n$ does not change appreciably; therefore, five iterations were always used in calculations, so that we assumed $\bar{f}_\infty = \bar{f}_5$.

The phase-space cell approximation leads to nonclassic critical exponents. Due to the approximations inherent to the method, however, the exponents are not exact and deviate slightly from the actual values. For example, for the critical exponents β, υ, and η, the phase-space cell approximation yields 0.34, 0.61, and 0 (Wilson, 1971b; Salvino and White, 1992), respectively, while the best theoretical estimates for these values are 0.325, 0.63, 0.0315 (Le Guillou and Zinn-Justin, 1977). These small deviations, however, are not important for most chemical engineering applications.

Calculation Method

Integration procedure

Equations 13–15 were applied at constant temperature. For each $\bar{\rho}$ between 0 and $\bar{\rho}_{\max}$ the following steps are performed:

- The initial values $\bar{f}_0$, $\bar{f}_{0,a}$ are calculated by Eqs. 15;
- K_n, $\tilde{f}_{n,l}$, $\tilde{f}_{n,s}$, $Q_{n,i}$, $\delta\bar{f}_n$ are evaluated by Eqs. 13, 14, and 15 until $n = 5$;
- The corrections to the dimensionless chemical potential and pressure $\bar{\mu}_{\text{cubic}}$ and $\bar{P}_{\text{cubic}}$ are computed from the thermodynamic relations:

$$\delta\bar{\mu} = \frac{\partial(\delta\bar{f})}{\partial\bar{\rho}} \tag{16}$$

$$\delta\bar{P} = \bar{\rho}(\delta\bar{\mu}) - \delta\bar{f}. \tag{17}$$

The integral in Eq. 14 is evaluated using the trapezoid rule.

In Figure 2 an example of the RG correction for propylene is reported, where the calculation is performed at saturated liquid density for three reduced temperatures. From Figure 2 it is clear that:

- The contribution of density fluctuations to Helmholtz energy density quickly decreases with n: five iterations are always enough to capture the total effect due to density fluctuations. This implies that shorter wavelength fluctuations, whose effect is evaluated at lower n values, give greater contribution to the correction.
- The overall correction, that is, the difference between the initial and asymptotic values, is stronger at higher reduced temperature, as when approaching the critical point.
- The Helmholtz energy approaches the asymptotic value more swiftly at low reduced temperature and more slowly near the critical point. This result is reasonable: only fluctuations with wavelengths less than the correlation length, ξ, are expected to give an appreciable contribution to the free energy of fluids and ξ is small far from the critical region, while $\xi \rightarrow \infty$ as $T_r \rightarrow 1$.

Evaluation of parameters

The value of parameter $\bar{c}_{RG}$ is determined by fitting the calculated critical compressibility factor, Z_c, which is given by

$$Z_c = \bar{P}_c/\bar{T}_c\,\bar{\rho}_c, \tag{18}$$

to its experimental value.

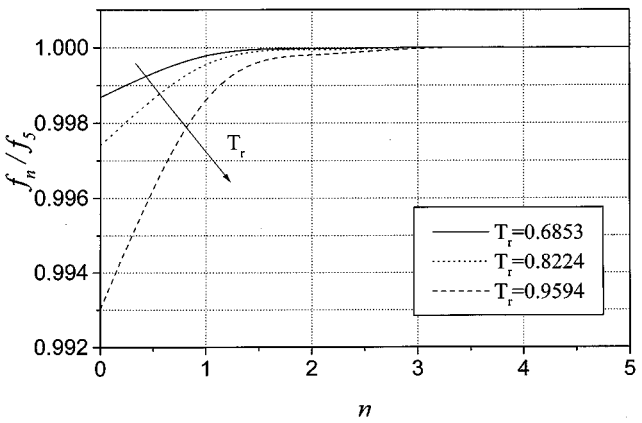

Figure 2. Variation in the specific Helmholtz energy final value of propylene with the iterative RG-step number *n* for three isotherms of RKS EOS.

(i) $T_r = 0.6853$ (solid line); (ii) $T_r = 0.8224$ (dotted line); (iii) $T_r = 0.9594$ (dashed line) (all calculations are performed at saturated liquid density).

Equation 18 requires the values of the dimensionless critical constants $\bar{\rho}_c$, $\bar{T}_c$, $\bar{P}_c$ that are not known *a priori*, because they are embedded in the cubic EOS parameters corrected by the RG method, see Eq. 10. Therefore, their values are obtained as follows:

- $\bar{T}_c$ is determined as the lowest temperature where the curve $\bar{P}(\bar{\rho})$ does not show slope inversion;
- $\bar{\rho}_c$ is calculated at the minimum of the function $(\partial\bar{P}/\partial\bar{\rho})_T$ at $T = T_c$. The derivative is obtained numerically;
- $\bar{P}_c$ is evaluated from the corrected cubic EOS, Eq. 9, at $\bar{T} = \bar{T}_c$, $\bar{\rho} = \bar{\rho}_c$.

Note that for $\bar{P}_c$ the knowledge of (corrected) parameter $\bar{c}$ is also required (cf. Eq. 9); hence, the calculation of $\bar{c}_{RG}$ and of $\bar{c}$ must be performed simultaneously. For details we refer to Appendix B. Note also that the values of parameters a_c, b, and c are changed as a result of the application of the RG procedure, as outlined in the same Appendix.

The value of parameter Δ was arbitrarily set equal to 1. We found that $\Delta = 1$ works better than other choices: in particular, the average error in term of root-mean-square deviation (RMSD) of saturated liquid density with respect to experimental values is minimized for many compounds if $\Delta = 1$.

Calculation of two-phase equilibrium curve

Once the parameters a_c, b, c, d, and $\bar{c}_{RG}$ are available, the saturated liquid and vapor densities can be calculated at any temperature, provided that the corresponding value of α is known. This can be obtained by solving the following equations:

$$\begin{cases} \bar{\mu}(\bar{\rho}_L) = \bar{\mu}(\bar{\rho}_V) \\ \bar{P}(\bar{\rho}_L) = \bar{P}(\bar{\rho}_V) = \bar{P}^{\text{sat}}_{\text{exp}} \end{cases} \tag{19}$$

with respect to α, $\bar{\rho}_L$, and $\bar{\rho}_V$, which are the dimensionless values of densities of the liquid and vapor phases at equilibrium. The corresponding dimensional densities are evaluated by reversing Eq. 10:

$$\rho_i = \frac{\bar{\rho}_i}{b} \qquad i = L, V. \tag{20}$$

An example of calculation is given in Figure 3 for propylene. It is clear that the proposed method is able to reproduce with high accuracy the experimental points of the saturation line. Also, it is noteworthy that the $P-v$ equilibrium curve obtained by the RG corrected EOS does not match exactly the one provided by the original cubic EOS even at lower temperature. This is so because the RG method modifies the original (dimensional) parameters of the EOS. Hence, we can distinguish two main contributions of the total correction coming from the application of the RG method:

1. One due to the change of the original values of the EOS parameters a_c, b, and c;
2. The other due to the calculation of the effect of density fluctuations, which is determined by $\bar{c}_{RG}$.

Figure 3 clearly shows that the first contribution to the EOS correction prevails at low temperature, while the flattening of equilibrium curve near the critical point comes from the second contribution.

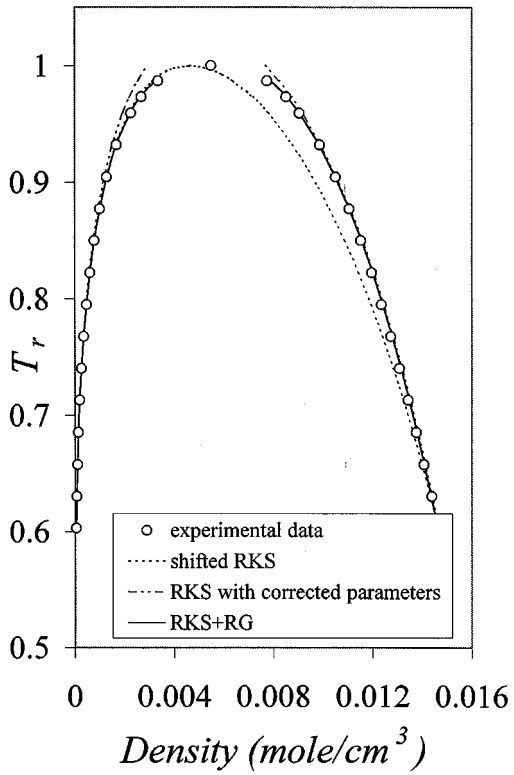

Figure 3. Vapor–liquid equilibrium curve for propylene.

(i) Experimental data (open circles); (ii) shifted RKS EOS (dotted line); (iii) shifted RKS EOS with corrected values of parameters a, b, c (dashed line); and (iv) shifted RKS EOS with RG correction (solid line).

Calculation of density outside the vapor – liquid equilibrium curve

If the parameters a_c, b, c, d, and $\bar{c}_{RG}$ are known, and the value of α at the given temperature is calculated by means of Eqs. 19 to reproduce the corresponding vapor-pressure value, it is possible to find the value of ρ at given T, P from the condition:

$$\bar{P}(\bar{\rho}) = \bar{P} \tag{21}$$

by directly applying the RG method (Eqs. 13–15).

Results and Discussion

In order to validate the currently proposed method, we decided to deal mainly with saturated liquid densities, for which more data are available. In addition, this is an important property where cubic EOSs perform poorly, as shown previously in Figure 1. As database a wide collection of pure fluids (polar and nonpolar, linear, and branched) was considered. The sources of data for density and vapor pressures used are summarized in Table 2.

Saturated liquid

The comparison with experimental data is done on the basis of the RMSD, defined as:

Table 2. Database of Compounds and Source of Data for Density and Vapor Pressure

Family	Compound	Saturated Liquid Density	Vapor Pressure
Alkanes	Methane	API 44	Ambrose and Walton (1989)
	Ethane	API 44	Reid et al. (1988)
	Propane	API 44	Ambrose and Walton (1989)
	n-Butane	API 44	Ambrose and Walton (1989)
	i-Butane	API 44	Reid et al. (1988)
	n-Pentane	API 44	Ambrose and Walton (1989)
	i-Pentane	API 44	Reid et al. (1988)
	n-Hexane	API 44	Ambrose and Walton (1989)
	n-Heptane	API 44	Amrbose and Walton (1989)
	n-Octane	API 44	Ambrose and Walton (1989)
	n-Nonane	API 44	Ambrose and Walton (1989)
	n-Decane	API 44	Ambrose and Walton (1989)
	n-Dodecane	API 44	Ambrose and Walton (1989)
Alkenes	Ethylene	Perry and Green (1984)	Reid et al. (1988)
	Propylene	Perry and Green (1984)	Reid et al. (1988)
Alkines	Acetylene	Perry and Green (1984)	Reid et al. (1988)
Dienes	1,3-Butadiene	Daubert and Danner (1993)	Reid et al. (1988)
Alcohols	Methanol	Perry and Green (1984)	Reid et al. (1988)
	Ethanol	API 44 Daubert and Danner (1993)	Reid et al. (1988)
	1-Propanol	API 44 Daubert and Danner (1993)	Reid et al. (1988)
	2-Propanol	API 44	Reid et al. (1988)
	n-Butanol	API 44 Daubert and Danner (1993)	Reid et al. (1988)
	2-Butanol	API 44	Reid et al. (1988)
Amine	Methylamine	API 44	Reid et al. (1988)
	Ethylamine	API 44	Reid et al. (1988)
Carboxylic acids	Acetic	API 44	Reid et al. (1988)
	Propionic	Daubert and Danner (1993)	Daubert and Danner (1993)
	n-Butyric	API 44	Reid et al. (1988)
Ketones	Methyl-*n*-propyl	Daubert and Danner (1993)	Daubert and Danner (1993)
Esters	Methyl acetate	Daubert and Danner (1993)	Reid et al. (1988)
	n-Propyl prop.	Daubert and Danner (1993)	Reid et al. (1988)
Aromatic compounds	Aniline	API 44	Reid et al. (1988)
	Chlorobenzene	API 44	Reid et al. (1988)

$$\mathrm{RMSD} = \sqrt{\frac{\sum_{i=1}^{npt} \mathrm{err}_i^2}{npt}} \tag{22}$$

$$\mathrm{err}_i = \frac{\rho_i^{\mathrm{calc}} - \rho_i^{\mathrm{exp}}}{\rho_i^{\mathrm{exp}}} \tag{23}$$

We present a result summary of calculations for all three classic cubic EOSs in Table 3, together with the investigated reduced temperature ranges.

It appears that the application of the currently proposed method is able to provide accurate predictions of saturated liquid densities in all the cases considered: the RMSD values are reduced to 0.3–6%. In particular, the characteristic error is 2–6% for alcohols and amines, 0.5–2% for alkanes, $<1\%$ for the two alkenes considered, 1–2% for esters and aromatic compounds, and 1–3% for carboxylic acids. Note that RMSD values obtainable in the same ranges by the same cubic EOS with the volume shift but without the RG correction are generally higher than 10%.

From Table 3, one can see also that among the different EOSs, best results are obtained with the vdW EOS and RKS EOS; the PR EOS is slightly less accurate. However, the agreement with the experimental densities is very good anyway.

Two examples of error plots are given in Figures 4 and 5 for the vdW EOS in the cases of methanol and acetic acid, respectively. These curves confirm the remarkable improvement provided by our method. The shape of the error curves is similar for all compounds considered, with a minimum between $T_r = 0.9$ and $T_r = 1$. The maximum deviation is always less than 5%, while it may also reach 50% without the RG correction. Recall that the $\bar{c}_{RG}$ parameter was fitted to the critical compressibility value, so that the error is zero at the critical point. The curves do not reach the critical temperature due to convergence problems.

We point out that such results were obtained by adding only one parameter to the original EOS. Of course, with our method the EOSs are no longer cubic and no longer analytical.

Discussion about parameters

In Figure 6 we plot the values of the $\bar{c}_{RG}$ parameter for different compounds and EOSs, obtained by the application

Table 3. RMS Deviation in Calculating Saturated Liquid Density for the van der Waals (vdW), Redlich–Kwong–Soave (RKS), and Peng–Robinson (PR) Equations

Family	Compound	Range of T_r	$RMSD^{vdW}$	$RMSD^{RKS}$	$RMSD^{PR}$
Alkanes	Methane	0.5938 ÷ 0.9734	0.01018	0.01054	0.01199
	Ethane	0.6324 ÷ 0.9836	0.01754	0.01785	0.01876
	Propane	0.6304 ÷ 0.9820	0.01789	0.01806	0.01784
	n-Butane	0.6425 ÷ 0.9718	0.01163	0.01218	0.01249
	i-Butane	0.6693 ÷ 0.9633	0.01880	0.01860	0.01617
	n-Pentane	0.6241 ÷ 0.9648	0.00448	0.00481	0.00801
	i-Pentane	0.6367 ÷ 0.9843	0.01115	0.01199	0.01485
	n-Hexane	0.5778 ÷ 0.9720	0.01459	0.01495	0.01574
	n-Heptane	0.5426 ÷ 0.9683	0.01722	0.01741	0.01729
	n-Octane	0.5154 ÷ 0.9726	0.01843	0.01892	0.02016
	n-Nonane	0.4930 ÷ 0.9755	0.01501	0.01313	0.01390
	n-Decane	0.4747 ÷ 0.9767	0.01491	0.01605	0.02238
	n-Dodecane	0.4454 ÷ 0.9771	0.02468	0.02514	0.03040
Alkenes	Ethylene	0.6021 ÷ 0.9739	0.00818	0.00833	0.01152
	Propylene	0.6305 ÷ 0.9731	0.00316	0.00347	0.00587
Alkines	Acetylene	0.6516 ÷ 0.9731	0.01293	0.01332	0.01419
Dienes	1,3-Butadiene	0.6588 ÷ 0.9765	0.00762	0.00833	0.01102
Alcohols	Methanol	0.5718 ÷ 0.9753	0.02235	0.02394	0.02951
	Ethanol	0.5404 ÷ 0.8818	0.01198	0.01188	0.01011
		0.7394 ÷ 0.9827	0.04701	0.04930	0.05676
	1-Propanol	0.5461 ÷ 0.8442	0.00829	0.00760	0.00459
		0.7079 ÷ 0.9780	0.04775	0.04901	0.05221
	2-Propanol	0.5767 ÷ 0.8718	0.01909	0.01865	0.01517
	n-Butanol	0.5206 ÷ 0.7515	0.00092	0.00120	0.00664
		0.7104 ÷ 0.9768	0.03954	0.03985	0.03864
	2-Butanol	0.5469 ÷ 0.7707	0.01061	0.00992	0.00618
Amine	Methylamine	0.6120 ÷ 0.9841	0.05688	0.05727	0.05718
	Ethylamine	0.6423 ÷ 0.9710	0.02297	0.02312	0.02217
Carboxylic acids	Acetic	0.5268 ÷ 0.9726	0.00988	0.01347	0.03060
	Propionic	0.6990 ÷ 0.9820	0.03007	0.03317	0.04501
	n-Butyric	0.5942 ÷ 0.8490	0.01326	0.01456	0.02218
Ketones	Methyl-*n*-propyl	0.6773 ÷ 0.9803	0.04442	0.04268	0.03839
Esters	Methyl acetate	0.6712 ÷ 0.9772	0.01768	0.01854	0.02017
	n-Propyl prop.	0.7035 ÷ 0.9849	0.01257	0.01356	0.01989
Aromatic compounds	Aniline	0.5625 ÷ 0.9773	0.02385	0.02536	0.03095
	Chlorobenzene	0.5584 ÷ 0.9537	0.01367	0.01371	0.01320

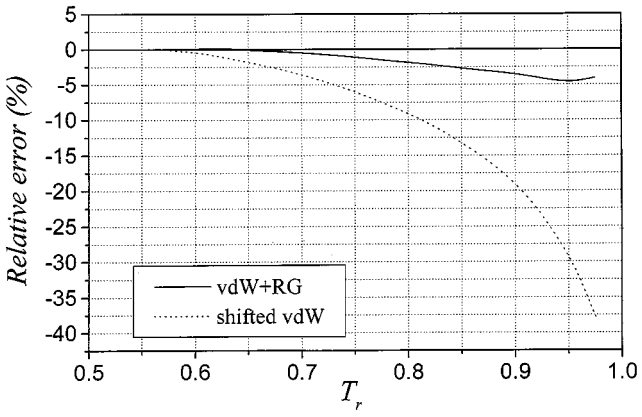

Figure 4. Relative percent error in the prediction of saturated liquid densities of methanol.

(i) By shifted vdW (dotted line) and (ii) by vdW with RG correction (vdW + RG, solid line).

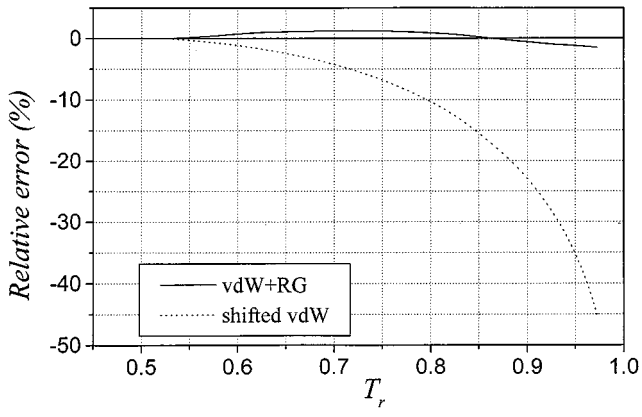

Figure 5. Relative percent error in the prediction of saturated liquid densities of acetic acid.

(i) By shifted vdW (dotted line) and (ii) by vdW with RG correction (vdW + RG, solid line).

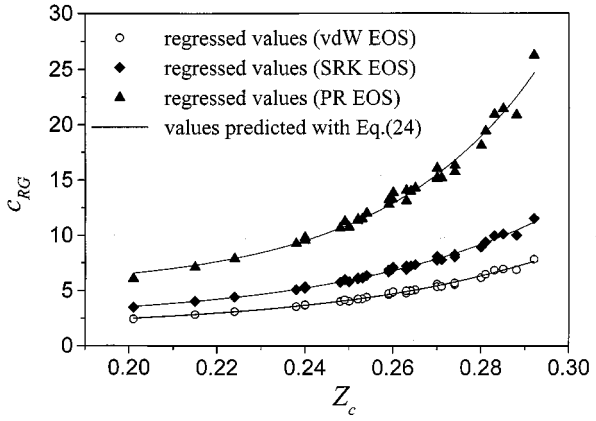

Figure 6. Correlation $\bar{c}_{RG}-Z_c$ for the classic cubic equations of state.

(a) van der Waals, (b) Redlich–Kwong–Soave, and (c) Peng–Robinson. The symbols represent regressed values of parameter $\bar{c}_{RG}$; the solid lines show the values calculated by Eq. 24.

of the RG method with $\Delta = 1$, as a function of the critical compressibility factor Z_c. It is interesting to note that there is a correlation between $\bar{c}_{RG}$ and Z_c. This is not surprising, since $\bar{c}_{RG}$ is a correction for density fluctuations, which primarily determines the value of Z_c. The following exponential functions were fitted to the curves:

$$\begin{aligned}
\bar{c}_{RG} &= 1.55914 + 0.01236 \exp\left(Z_c/0.04677\right) && \text{for vdW EOS} \\
\bar{c}_{RG} &= 2.30017 + 0.02119 \exp\left(Z_c/0.04878\right) && \text{for RKS EOS} \\
\bar{c}_{RG} &= 5.11820 + 0.004424 \exp\left(Z_c/0.03479\right) && \text{for PR EOS}
\end{aligned} \tag{24}$$

From Figure 6 we note that

- $\bar{c}_{RG}$ values for the same EOS decrease as Z_c decreases;
- $\bar{c}_{RG}$ for the same compound increases as we pass from vdW to RKS to PR EOS.

Both results are reasonable if we think that the $\bar{c}_{RG}$ parameter is an index of the extent of the RG correction: the less is $\bar{c}_{RG}$, the higher is $\delta \bar{f}_n$ (see Eqs. 13–15). Particularly, since the original PR EOS is more accurate for density calculations than RKS, and vdW is the worst one, we expect larger values of $\bar{c}_{RG}$ for PR EOS than for RKS EOS and for vdW EOS. Moreover, it is well known that cubic EOSs usually predict Z_c values higher than the experimental ones, so we expect that $\bar{c}_{RG}$ decreases as Z_c decreases. These findings are in agreement with White's statement: ''the compression ratio at the critical point is one measure of the aggregate size of the fluctuation contributions $\delta \bar{f}_n$''(White and Zhang, 1995).

Conclusions

The problem of evaluating pure fluid volumetric properties in the critical region by a cubic equation of state has been addressed. A renormalization group method has been developed for the application to a generalized cubic equation of state. In addition, a procedure to calculate model parameters has been outlined.

The proposed method has been used successfully to calculate saturated liquid densities of a wide collection of components of different polarity. The improvement of the performance of the cubic equations of state for this property is remarkable.

Notation

npt = number of points
δ = RG correction

Subscripts and superscripts

exp = experimental
n = iterative RG-step number
∞ = convergence value after infinite iterative steps
calc = calculated
sat = saturation

Literature Cited

Amrbose, D., and J. Walton, ''Vapor Pressures Up to Their Critical Temperatures of Normal Alkanes and 1-Alkanols,'' *Pure Appl. Chem*., **61**, 1395 (1989).

Anisimov, M. A., J. V. Sengers, and A. K. Wyczalkowska, ''Global Crossover Equation of State of a Van der Waals Fluids,'' Int. Conf. on Properties and Phase Equilibria for Product and Process Design, The Netherlands (1998a).

Anisimov, M. A., A. A. Povodyrev, and J. V. Sengers, ''Crossover Critical Phenomena in Complex Fluid,'' Int. Conf. on Properties and Phase Equilibria for Product and Process Design, The Netherlands (1998b).

American Petroleum Institute, ''Selected Values of Properties of Hydrocarbons and Related Compounds,'' American Petroleum Institute Research Project 44 (1972).

Daubert, T. E., and R. P. Danner, *Physical and Thermodynamics Properties of Pure Compounds: Data Compilation*, Taylor & Francis, New York (1993).

Goldenfeld, N., *Lectures on Phase Transition and the Renormalization Group*, Addison-Wesley, New York (1996).

Kiselev, S. B., ''Cubic Crossover Equation of State,'' *Fluid Phase Equilib*., in press (1998).

Kiselev, S. B., and D. G. Friend, ''Cubic Crossover Equation of State for Mixtures,'' *Fluid Phase Equilib*., **147**, 7 (1998).

Le Guillou, J. C., and J. Zinn-Justin, ''Critical Exponents for the n-Vector Model in Three Dimensions from Field Theory,'' **39**, 95 (1977).

Lue, L., and J. M. Prausnitz, ''Renormalization-Group Corrections to and an Approximate Free-Energy Model for Simple Fluids Near to and Far from the Critical Region,'' *J. Chem. Phys*., **108**, 5529 (1998a).

Lue, L., and J. M. Prausnitz, ''Thermodynamics of Phase Equilibria for Fluid Mixtures Near to and Far from the Critical Region,'' *AIChE J*., **44**, 1455 (1998b).

Perry, R. H., and D. Green, *Perry's Chemical Engineer's Handbook*, 6th ed., McGraw-Hill, New York (1984).

Peneloux, A., E. Rauzy, and R. Freze, ''A Consistent Correction for the Redlich Kwong Soave Volumes,'' *Fluid Phase Equilibria*, **8**, 7 (1982).

Reid, R., J. M. Prausnitz, and B. Poling, *The Properties of Gases and Liquids*, 4th ed., McGraw-Hill, New York (1988).

Salvino, L. W., and J. A. White, ''Calculation of Density Fluctuation Contributions to Thermodynamics Properties of Simple Fluids,'' *J. Chem. Phys*., **96**(6), 4559 (1992).

Soave, G., L. Sponchiado, and A. Bertucco, ''How to Use Simultaneously Different Cubic Equations of State to Improve the Calculation of Pure Component and Mixture Properties,'' in press (1999).

Soave, G., ''Direct Calculation of Pure Compound Vapor Pressures through Cubic Equations of State,'' *Fluid Phase Equilib*., **31**, 203 (1986).

Sponchiado, L., Thesis, Univ. of Padova (1998).

White, J. A., and S. Zhang, ''Renormalization Group Theory for Fluids,'' *J. Chem. Phys*., **99**(3), 2012 (1993).

White, J. A., and S. Zhang, ''Renormalization Theory of Nonuniversal Thermal Properties of Fluids,'' *J. Chem. Phys.*, **103**, 1922 (1995).
White, J. A., and S. Zhang, ''Renormalization Theory for Fluids to Greater Density Distances from the Critical Point,'' Symp. on Thermophysical Properties, Boulder, CO (1997).
Wilson, K. G., ''Renormalization Group and Critical Phenomena. I. Renormalization Group and the Kadanoff Scaling Picture,'' *Phys. Rev. B*, **4**, 3174 (1971a).
Wilson, K. G., ''Renormalization Group and Critical Phenomena. II. Phase-Space Cell Analysis of Critical Behavior,'' *Phys. Rev. B*, **4**, 3184 (1971b).

Appendix A: Calculation of $\bar{\mu}_{\text{cubic}}$ and $\bar{f}_{\text{cubic}}$

To calculate $\bar{\mu}_{\text{cubic}}$, we start from the thermodynamic relations:

$$\bar{\mu}_{\text{cubic}} = \bar{\mu}^{id} + \bar{\mu}^{r}$$
$$\bar{\mu}^{id} = \bar{\mu}^{0} + \bar{T}\ln\bar{P}$$
$$\bar{\mu}^{r} = \bar{T}\ln\varphi \qquad \text{(A1)}$$

where $\bar{\mu}^{id}$ is the ideal gas chemical potential, $\bar{\mu}^{0}$ is the reference chemical potential, $\bar{\mu}^{r}$ is the residual chemical potential.

The fugacity coefficient in Eq. A1 is evaluated by performing the integration

$$\ln\varphi = \int_0^P \frac{Z-1}{P}\,dP = \int_0^P \left(\frac{v}{RT} - \frac{1}{P}\right) dP. \qquad \text{(A2)}$$

With a suitable change of integration variable, we obtain

$$\ln\varphi = \frac{Pv}{RT} - 1 - \ln\frac{Pv}{RT} - \int_v^\infty \left(\frac{P}{RT} - \frac{1}{v}\right) dv. \qquad \text{(A3)}$$

Substituting Eq. 9 into the Eq. A3 and integrating, we find the dimensional form of fugacity coefficient:

$$\ln\varphi = \frac{Pv}{RT} - 1 - \ln\frac{Pv}{RT} - \ln\frac{(v+c-b)}{v} + \frac{a(T)}{dRT}\ln\left(\frac{v+c}{v+c+d}\right). \qquad \text{(A4)}$$

The dimensionless expression is obtained by introducing the definition of dimensionless variables (see Eq. 10):

$$\ln\varphi = \frac{\bar{P}}{\bar{T}\bar{\rho}} - 1 - \ln\frac{\bar{P}}{\bar{T}\bar{\rho}} - \ln\left[1+(\bar{c}-1)\bar{\rho}\right] + \frac{1}{\bar{d}\bar{T}}\ln\left[\frac{1+\bar{c}\bar{\rho}}{1+(\bar{c}+\bar{d})\bar{\rho}}\right]. \qquad \text{(A5)}$$

The chemical potential $\bar{\mu}_{\text{cubic}}$ is derived directly from Eq. A1:

$$\bar{\mu} = \bar{\mu}^{0} - \bar{T}\ln\left[1+(\bar{c}-1)\bar{\rho}\right] + \frac{1}{\bar{d}}\ln\left[\frac{1+\bar{c}\bar{\rho}}{1+(\bar{c}+\bar{d})\bar{\rho}}\right] - \frac{\bar{\rho}}{(1+\bar{c}\bar{\rho})\left[1+(\bar{c}+\bar{d})\bar{\rho}\right]} + \bar{T}\ln\bar{T}\bar{\rho} - \frac{(\bar{c}-1)\bar{\rho}\bar{T}}{1+(\bar{c}-1)\bar{\rho}}. \qquad \text{(A6)}$$

Note that the value of term $\bar{\mu}^{0}$ is unimportant, since $\bar{\mu}^{0}$ appears only in isofugacity equation.

The thermodynamic relation $\bar{f} = \bar{\rho}\bar{\mu} - \bar{P}$ allows an easy calculation of Helmholtz energy density $\bar{f}_{\text{cubic}}$:

$$\bar{f}_{\text{cubic}} = \bar{\rho}\left\{\bar{\mu}^{0} - \bar{T}\ln\left[1+(\bar{c}-1)\bar{\rho}\right] + \frac{1}{\bar{d}}\ln\left[\frac{1+\bar{c}\bar{\rho}}{1+(\bar{c}+\bar{d})\bar{\rho}}\right] + \bar{T}\left[\ln\left(\bar{T}\bar{\rho}\right)-1\right]\right\}. \qquad \text{(A8)}$$

Again, note that the value of term $\bar{\mu}^{0}$ is not of interest since it does not contribute to the RG correction, as can be seen from Eq. 14.

Appendix B: Iterative Procedure for Simultaneous Evaluation of Parameters $\bar{c}_{RG}$ and $\bar{c}$

The two-equation system is given by

$$Z_c^{\text{calc}} = Z_c^{\text{exp}}$$
$$\bar{\rho}^{\text{calc,ref}} = \bar{\rho}^{\text{exp,ref}} \qquad \text{(B1)}$$

where the superscript ref stands for the reference conditions at which the volume-shift parameter $\bar{c}$ has to be calculated.

The system (Eq. B1) is solved by applying a Newton–Raphson algorithm. Once the initial values for parameters $\bar{c}_{RG}$ and $\bar{c}$ are assumed, the errors on both equations in Eq. B1 have to be evaluated.

For the definition of the first error, the experimental value of Z_c is needed; note that $\bar{T}_c$, $\bar{\rho}_c$, and $\bar{P}_c$ can be calculated directly.

On the other hand, for the second equation error we need the experimental dimensionless densities $\bar{\rho}^{\text{exp}} = b\rho^{\text{exp}}$, and $\bar{\rho}^{\text{calc}}$ at $\bar{T}$, $\bar{P}$ values corresponding to dimensional temperature and pressure of reference density data. In order to do that, the parameters a and b corrected by the RG method must be determined according to Eq. 10. The calculation of a_c and b comes directly from the solution of the system:

$$\begin{cases} \bar{T}_c^{\text{calc}} = \dfrac{bRT_c^{\text{exp}}}{a_c} \\ \bar{P}_c^{\text{calc}} = \dfrac{b^2}{a_c}P_c^{\text{exp}}. \end{cases} \qquad \text{(B2)}$$

To evaluate the parameter α at the given reference temperature (the temperature for the density datum), we impose the condition:

$$P_{\text{calc}}^{\text{sat}} = P_{\text{exp}}^{\text{sat}}. \qquad \text{(B3)}$$

Since the RG method works with dimensionless variables, while the density data are dimensional, an iterative procedure must be followed:

1. An initial guess for the parameter α (e.g., the one for the EOS without correction) is taken;

2. $\bar{T}$ is calculated by definition, Eq. 10, with the initial value of α and with b obtained by solving the system, Eq. B2;

3. The RG method is applied to isotherm $\bar{T}$ in order to calculate the corrected $\bar{\mu}$, $\bar{P}$;

4. The dimensionless vapor pressure is calculated by imposing the conditions:

$$\begin{cases} \bar{\mu}(\bar{\rho}_L) = \bar{\mu}(\bar{\rho}_V) \\ \bar{P}(\bar{\rho}_L) = \bar{P}(\bar{\rho}_V). \end{cases} \tag{B4}$$

5. The dimensional value of calculated vapor pressure is determined by the definition of $\bar{P}$;

6. Equation B3 is checked for convergence; if this is not the case, parameter α is changed and the iterative steps are repeated.

Once convergence on α is achieved, it is possible to evaluate $\bar{\rho}^{\text{calc}}$, by solving the equation

$$\bar{P}(\bar{\rho}, \bar{T}) = \bar{P}^{\text{ref}}, \tag{B5}$$

where the reference $\bar{P}^{\text{ref}}$ can be derived from its dimensional value (usually 1 atm), because now the corrected parameters a and b are known.

At this point, the error of the second equation in Eq. B1 also can be calculated, and the Newton–Raphson algorithm can be applied to update the values of parameters $\bar{c}_{RG}$ and $\bar{c}$ until total convergence is obtained.

Manuscript received June 25, 1998, and revision received Dec. 14, 1998.